Molecular Transformations of Bicyclic Nitrogen Heterocycles on Triosmium Clusters

Shariff E. Kabir, Douglas S. Kolwaite, and Edward Rosenberg*

Department of Chemistry, The University of Montana, Missoula, Montana 59812

Lincoln G. Scott, Tim McPhillips, Ricardo Duque, Michael Day, and Kenneth I. Hardcastle

Department of Chemistry, California State University, Northridge, California 91330

Received September 8, 1995[⊗]

The reactions of indoline (I) and tetrahydroquinoline (THQ) with $Os_3(CO)_{10}(CH_3CN)_2$ (**1**) have been studied. Reaction of **1** with I at ambient temperatures gives $Os_3(CO)_{10}(\mu\text{-H})(\mu\text{-}\eta^2\text{-}C_8H_7NH)$ (**2**), which decarbonylates thermally to give a mixture of the tautomeric complexes $Os_3(CO)_9(\mu\text{-H})_2(\mu_3\text{-}\eta^2\text{-}C_8H_7N)$ (**3** and **4**) whose structures differ by having a μ-alkylidene−imino bonding mode (**3**) *vs* a μ-amido−aryl bonding mode (**4**). The conversion of **2** to **3** and **4** follows strictly first-order kinetics and the equilibrium constant K(**4**/**3**) = 6. Further thermolysis of **3** or **4** yields the dehydrogenated cluster $Os_3(CO)_9(\mu\text{-H})_2(\mu_3\text{-}\eta^2\text{-}C_8H_4\text{-}NH)$ (**5**). In the case of THQ reacting with **1**, no direct analog of **2** is observed but a directly analogous pair of tautomers $Os_3(CO)_9(\mu\text{-H})(\mu_3\text{-}\eta^2\text{-}C_9H_9N)$ (**6** and **7**) are obtained. In addition, the product $Os_3(CO)_{10}(\mu\text{-H})(\mu\text{-}\eta^1\text{-}C_9H_{10}N(CH_3)CN)$ (**8**) is obtained, which is the result of an apparent nucleophilic attack of THQ on the coordinated acetonitrile of **1**. Thermolysis of **7** yields the dehydrogenation product $Os_3(CO)_{10}(\mu\text{-H})(\mu\text{-}\eta^2\text{-}C_9H_8N)$ (**10**), which maintains the η^2-C(8)−N bonding to the metal core, in sharp contrast to **5**. Thermolysis of **8** yields $Os_3(CO)_8(\mu\text{-H})_2(\mu_3\text{-}\eta^2\text{-}C_9H_9N(CH_3)CN)$ (**11**) in which the acetonitrile nitrogen caps the trimetallic core and the C−H bond at C(8) has been activated. Reaction of **3** and **6** with CF_3SO_3H or CF_3CO_2H reveals reversible protonation at the nitrogen of the coordinated I or THQ. Protonation of **7** on the other hand takes place at the metal core but **7**H$^+$ gradually rearranges to **6**H$^+$ which yields **6** on deprotonation. The solid-state structures of **4**, **6**, and **10** are reported. In sharp contrast to the above results, isotetrahydroquinoline (ITHQ) reacts with **1** to give the μ-imidoyl cluster $Os_3(CO)_{10}(\mu\text{-H})(\mu\text{-}\eta^2\text{-}C_9H_8N)$ (**13**), which decarbonylates to give the μ_3-imidoyl cluster $Os_3(CO)_9(\mu\text{-H})(\mu_3\text{-}\eta^2\text{-}C_9H_8N)$ (**14**). The thermal behavior and dynamics of these complexes are discussed in the context of current models for hydrodenitrification.

Introduction

There has been considerable progress in recent years in our understanding of the factors controlling the rates of hydrodenitrification (HDN) of aromatic nitrogen heterocycles.[1] Both heterogeneous[2] and homogeneous[3] catalytic studies have shown that the first step in the HDN process for quinoline (Q) and isoquinoline (IQ) is reduction of the heteroaromatic ring. The enhancement of the rate of HDN by sulfided catalyst surfaces resulting from composite hydrodesulfurization (HDS) and HDN has been explained by invoking surface-bound sulfur in an S_N2 carbon−nitrogen bond cleavage process.[4] The requirement of a protic acid in many industrial HDN catalysts has been rationalized by an operative E2 carbon−nitrogen bond cleavage process. Carbon−nitrogen bond cleavage at ambient temperatures has been achieved by hydride reduction of the sterically encumbered nitrogen heterocycle 2,4,6-tri-*tert*-butylpyridine complexed to a mononuclear tantalum center.[5] This same tantalum center undergoes an η^1 to η^2 transformation on coordination of Q followed by reduction of the heteroaromatic ring but without carbon−nitrogen bond cleavage.[5] Metal cluster complexes have proved to be valuable for modeling carbon−oxygen[6] bond cleavage processes at metal surfaces, yet reactions of metal carbonyl clusters with HDN substrates such as Q, tetrahydroquinoline (THQ), and isotetrahydroquinoline (ITHQ) at elevated temperatures lead to products in which the heteroaromatic ring has been dehydrogenated.[7] Kinetic modeling of the HDN process indicates that dehydrogenation of substrates such as THQ can

[⊗] Abstract published in *Advance ACS Abstracts,* March 1, 1996.

(1) See symposium: Mechanism of HDS/HDN Reactions. *Prepr., ACS Div. of Pet. Chem.* **1988**, *33*, 638−717.

(2) Gates, B. C. *Catalytic Chemistry*; J. Wiley and Sons: New York, 1992; p 409.

(3) Fish, R. H. In *Aspects of Homogeneous Catalysts;* Ugo, R., Ed.; Kluwer Academics: Dordrecht, The Netherlands, 1990; pp 65−83.

(4) (a) Satterfield, C. N.; Gultekin, S. *Ind. Eng. Chem., Proc. Des. Dev.* **1981**, *20*, 62. (b) Yang, S. H.; Satterfield, C. M. *J. Catal.* **1983**, *81*, 62. (c) Yang, S. H.; Satterfield, C. N. *Ind. Eng. Chem., Proc. Des. Dev.* **1984**, *23*, 20. (d) Brunet, S.; Perot, G. *React. Kinet. Catal. Lett.* **1985**, *29*, 15. (e) Satterfield, C. N.; Smith, C. M.; Ingalls, M. *Ind. Eng. Chem., Proc. Des. Dev.* **1985**, *24*, 1000. (f) Vivier, L.; D'Araujo, P.; Kasztelan, S.; Perot, G. *Bull. Soc. Chim. Belg.* **1991**, *100*, 807.

(5) (a) Gray, S. D.; Smith, D. P.; Bruck, M. S.; Wigley, D. E. *J. Am. Chem. Soc.* **1992**, *114*, 5462. (b) Gray, S. D.; Fox, P. A.; Kingsborough, M. S.; Bruci, M. S.; Wigley, D. E. *Prepr., ACS Div. Pet. Chem.* **1993**, *38*, 706.

(6) Horvath, I.; Adams, R. D. *Prog. Inorg. Chem.* **1985**, *33*, 127.

(7) (a) Eisenstadt, A.; Giandomenico, C. M.; Frederick, M. F.; Laine, R. M. *Organometallics* **1985**, *4*, 2033. (b) Laine, R. M. *New J. Chem.* **1987**, *11*, 543.

0276-7333/96/2315-1979$12.00/0

be competitive with carbon-nitrogen bond cleavage even in the presence of hydrogen.[2] In light of the fact that it was recently demonstrated that carbon-nitrogen bond cleavage can be accomplished catalytically at 150 °C[8] and stoichiometrically at ambient temperatures[9] with aliphatic amines using triosmium clusters, we thought it would be useful to reexamine the reactions of HDN precursors such as THQ, ITHQ, and I with the lightly stabilized triosmium cluster $Os(CO)_{10}(CH_3CN)_2$ (**1**). The purpose of these initial studies was not to accomplish HDN but rather to understand the sequence of C−H and N−H bond activation processes after reduction of the heteroaromatic ring and to understand which bonding modes of these heterocycles, if any, are resistant to dehydrogenation. These studies have yielded a series of structurally related complexes whose thermal chemistry and behavior toward protic acids are reported herein.

Results

A. Reaction of Indoline with $Os_3(CO)_{10}(CH_3CN)_2$. The reaction of indoline (**I**) with **1** at ambient temperatures in dry benzene over 20 h yields a single major product in 67% isolated yield. The product was characterized by infrared, ^{1}H-NMR, and elemental analysis and shown to be $Os_3(CO)_{10}(\mu\text{-H})(\mu\text{-}\eta^2\text{-}C_8H_7NH)$ (**2**) (eq 1).

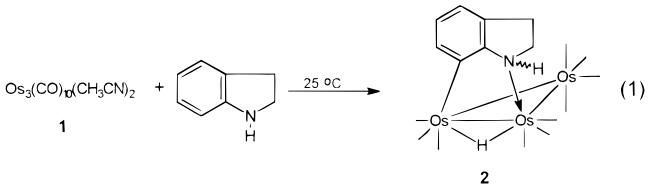

The compound exists as two isomers in solution which differ by the disposition of the N−H bond relative to the cluster (Scheme 1) as evidenced by the presence of

Scheme 1. Isomers of 2

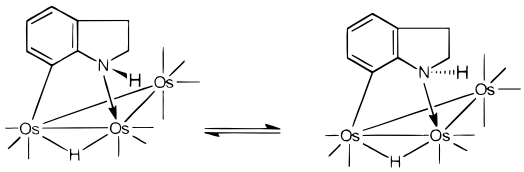

two N−H resonances at 4.15 and 4.05 ppm and two hydride resonances at −13.59 and −13.80 ppm both in 2.5:1 ratio. Companion resonances for the hydrocarbon CH and CH_2 groups are also seen but are only partially resolved. Exchange between these isomers is slow on the NMR time scale as previously observed for related isomers of *N*-methylpyrrolidine bound to triosmium clusters.[10] The reaction of indoline with **1** at 60 °C for 8 h yields two major products characterized by infrared, ^{1}H-NMR, and elemental analysis, $Os_3(CO)_9(\mu\text{-H})_2(\mu_3\text{-}\eta^2\text{-}C_8H_7N)$ (**3**) and $Os_3(CO)_9(\mu\text{-H})_2(\mu_3\text{-}\eta^2\text{-}C_8H_7N)$ (**4**) in 30 and 22% isolated yields, respectively. Compound **3** is deep red and is apparently an isomer of **4** which has the characteristic yellow color of most triosmium complexes (eq 2).

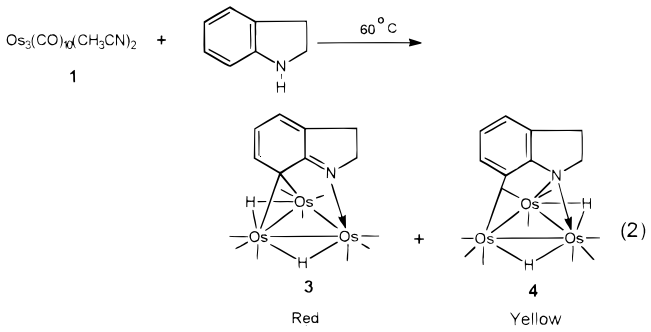

Compound **3** is completely rigid on the NMR time scale up to +90 °C. ($\Delta G^{\ddagger} > 72$ kJ/mol) as evidenced by the onset of slight reversible broadening of the two hydride resonances at this temperature. Compound **4** on the other hand shows a fluxional behavior which indicates hydride exchange in the temperature range examined. Thus at −50 °C we observe two sharp hydride resonances at −13.83 and −13.92 ppm and four aliphatic resonances at 3.88, 3.46, 3.19, and 2.92 ppm, all of equal relative intensity. At room temperature, a single sharp hydride resonance at −13.86 ppm is observed while the aliphatic resonances average to two broadened resonances at 3.67 and 3.09 ppm. The aromatic resonances remain unchanged through this temperature range at 7.21, 6.61, and 6.51 ppm. This behavior is consistent with a process in which one of the hydrides moves from edge-to-edge to induce a symmetry plane followed by edge-to-edge migration of either hydride (Scheme 2).[11] Only one of two distin-

Scheme 2. Hydride Exchange in 4 and 6

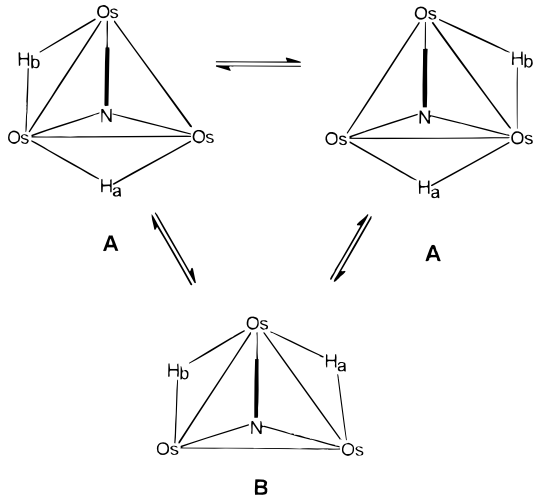

guishable isomers (isomer A, Scheme 2) of **4** is detectable at the low-temperature limit.

The thermolysis of **2** at 60 °C follows strictly first-order kinetics converting to **3** and **4** (eq 3). The rate constant for this conversion is $(1.8 \pm 0.2) \times 10^{-5}$ s^{-1}, and both isomers of **2** appear to convert at equal rates. Isolated **3** in turn converts to **4** at 100 °C with an approximate half-life of 3 h. Further prolonged thermolysis of **4** at 128 °C in octane leads to $Os_3(\mu\text{-H})_2(\mu_3$-

(8) Adams, R. D.; Babin, J. E.; Tanner, J. T.; Wolfe, J. A. *J. Am. Chem. Soc.* **1990**, *112*, 3426.
(9) Kabir, S. E.; Day, M.; Irving, M.; McPhillips, T.; Minassian, H.; Rosenberg, E.; Hardcastle, K. I. *Organometallics* **1991**, *10*, 3997.
(10) (a) Day, M. W.; Hajela, S.; Kabir, S. E.; Irving, M.; McPhillips, T.; Wolf, E.; Hardcastle, K. I.; Rosenberg, E.; Milone, L.; Gobetto, R.; Osella, D. *Organometallics*, **1991**, *10*, 2743. (b) Rosenberg, E.; Day, M.; Espitia, D.; Hardcastle, K. I.; Kabir, S. E.; McPhillips, T.; Gobetto, R.; Milone, L.; Osella, D. *Organometallics* **1993**, *12*, 2390.
(11) Keister, J. B.; Frey, V.; Zbinden, D.; Merbach, A. E. *Organometallics* **1991**, *10*, 1497 and references therein.

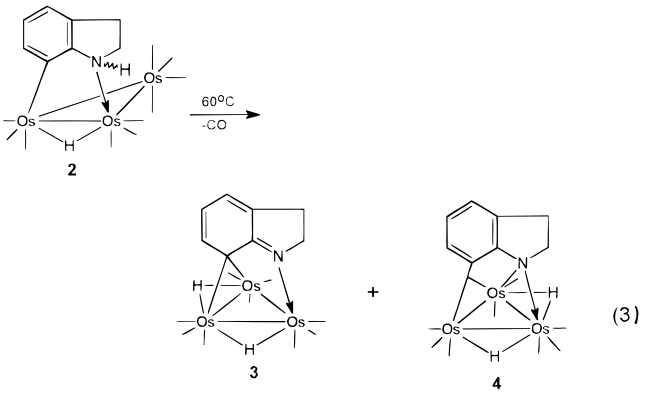

η^2-$C_8H_4NH)(CO)_9$ (**5**) originally synthesized by the reaction of indole with $Os_3(CO)_{12}$ (eq 4).[12] Compounds

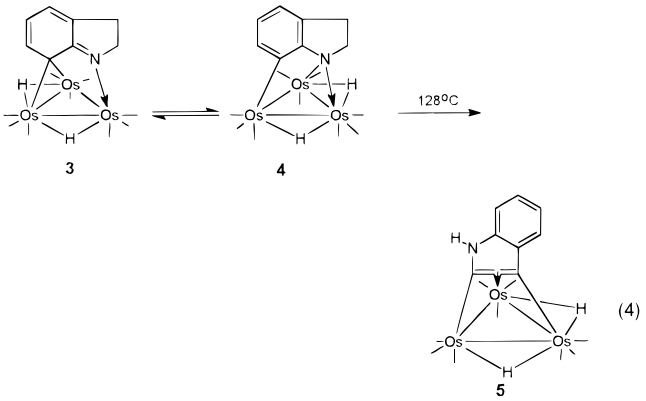

3 and **4** appear to be involved in a tautomeric (*vide infra*) equilibrium since heating of **3** (>20 h) at 100 °C results in a constant ratio of **4:3** of 6.1:1 and heating **4** results in the same ratio. Only trace amounts of other compounds appear during these thermolyses.

B. Reaction of Tetrahydroquinoline with $Os_3(CO)_{10}(CH_3CN)_2$. The reaction of THQ with **1** at 25−60 °C in methylene chloride or benzene does not lead to a compound analogous to **2**. Instead, four compounds are isolated: $Os_3(CO)_9(\mu\text{-H})_2(\mu_3\text{-}\eta^2\text{-}C_9H_9N)$ (**6**) directly analogous to **3**; $Os_3(CO)_9(\mu\text{-H})(\mu_3\text{-}\eta^2\text{-}C_9H_9N)$ (**7**) directly analogous to **4**; $Os_3(CO)_{10}(\mu\text{-H})(\mu\text{-}\eta^1\text{-}C_9H_9N(CH_3)CN)$ (**8**) and $Os_3(CO)_{10}(\mu\text{-H})(\mu\text{-}\eta^2\text{-}C_9H_6N)$ (**9**). These compounds were characterized by ^1H and ^{13}C-NMR, infrared, and elemental analysis. In the case of **8** and **9**, attached proton test (APT), one-dimensional ^{13}C, and two-dimensional ^1H COSY experiments allowed complete assignment of all but the carbonyl resonances in these compounds (eq 5). Depending on the temperature and reaction time, **6** is obtained in 22−31% yield. As for **3** and **4**, **6** and **7** are related by a tautomeric equilibrium for which the equilibrium ratio of **7:6** is similar to that of **4:3**, being 6:1. Interestingly, the rate of equilibration is significantly slower than in the case of **3** converting to **4** having a half-life of 8.3 h. Like **3**, **6** is structurally rigid on the NMR time scale and is deep red, while **7** is fluxional on the NMR time scale like **4**. In contrast to **4** however, **7** shows the presence of two isomers at the low-temperature limit as evidenced by the presence of a low-intensity hydride signal at −80 °C (Figure 1) and the differential line broadening of the two hydride signals as the temperature is increased. This implies some significant population of the more symmetrical

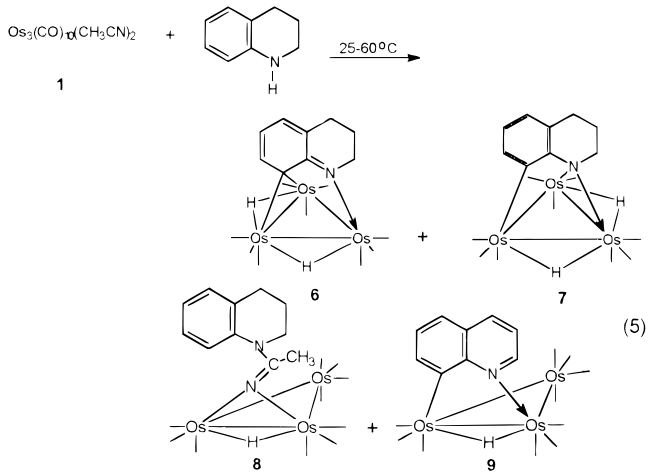

isomer B (Scheme 2). Although the exchange pathway observed for **4** and **7** is well-known for these types of clusters, the observation of the single hydride resonance representing the symmetrical intermediate is unusual.[11]

Thermolysis of **7** in refluxing octane for 24−48 h yields $Os_3(CO)_9(\mu\text{-H})(\mu\text{-}\eta^2\text{-}C_9H_8N)$ (**10**) as the only isolable product in addition to nonspecific decomposition (eq 6). The assignment of the structure of **10** is based

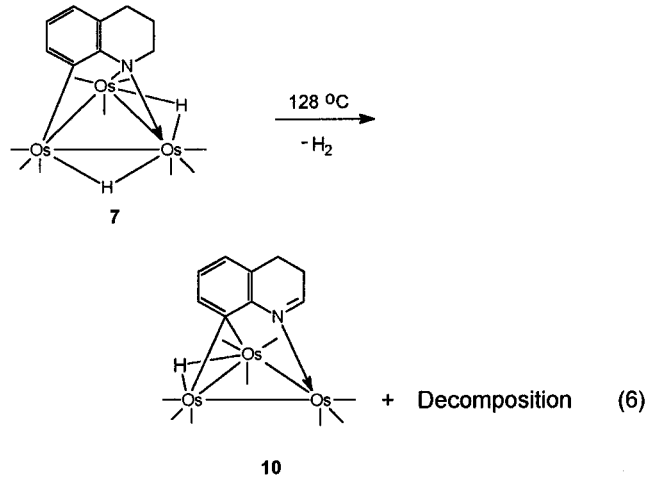

on the observation of a doublet of doublets at 8.85 ppm which correlates (2D-^{1}H-COSY) only with one of the aliphatic methylene resonances at 2.85 ppm, while the three other resonances in the aromatic region correlate with each other. This connectivity pattern is only consistent with the ligand structure proposed for **10**. Compounds **10** and **5** represent dehydrogenation products relative to **7** and **4**, respectively, but the nitrogen atom remains coordinated to the cluster.

The formation of **8** represents a completely novel transformation on a trinuclear cluster where THQ has apparently attacked a coordinated acetonitrile and is reminiscent of the well-known attack of amines on coordinated carbon monoxide to yield $\mu\text{-}\eta^2$-carboamyl derivatives.[13] Thermolysis of **8** at 128 °C in octane yields two compounds: $Os_3(CO)_8(\mu\text{-H})(\mu_3\text{-}\eta^2\text{-}C_9H_9N\text{-}(CH_3)CN)$ (**11**) and $Os_3(CO)_9(\mu\text{-H})(\mu_3\text{-}\eta^2\text{-}C_9H_8N)$ (**12**) in 45 and 23% yields, respectively (eq 7). The structure of **12** ,which is directly related to the previously reported decacarbonyl imidoyl derivative of Q,[7] is based on ^1H and ^{13}C-NMR and shows the typical VT ^1H-NMR

(12) Hardcastle, K. I.; Minassian, H.; Arce, A. J.; DeSanctis, Y.; Deeming, A. J. *J. Organomet. Chem.* **1989**, *368*, 119.

(13) Mayr, A.; Lin, Y. C.; Boog, N. M.; Kaesz, H. D. *Inorg. Chem.* **1984**, *23*, 4640.

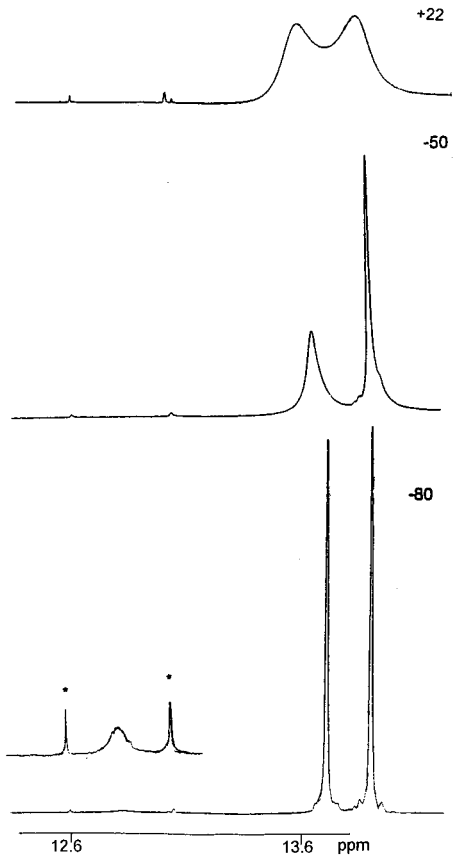

Figure 1. VT ^{1}H-NMR of the hydride region of **7** at 400 MHz in CD_2Cl_2 (the asterisks indicate traces of **6**).

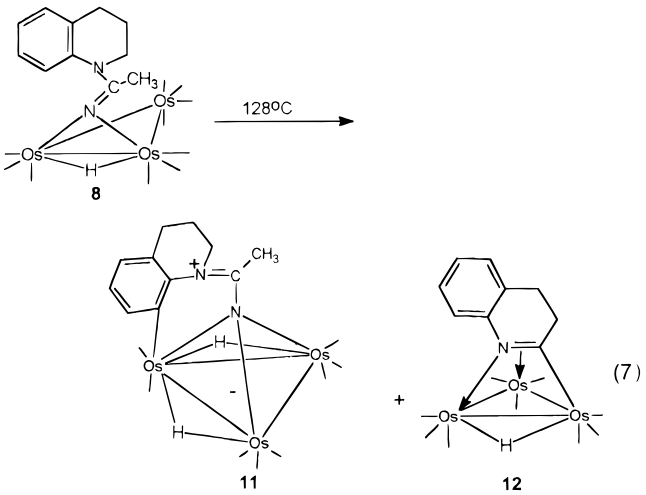

associated with μ_3-imidoyl clusters (i.e., the windshield wiper motion).[10] The structure of **11** is based on elemental analysis and infrared and ^{1}H NMR spectroscopy and was confirmed by a solid-state structure (*vide infra*).

C. Solid-State Structures of 6, 4, and 10. The solid-state structure of **6**, the red tautomer of the THQ pair, is shown in Figure 2, crystal data are given in Table 1, selected bond distances and angles are given in Table 2, and atomic coordinates are given in Table 3. We will discuss this structure first since it is representative of the kinetic products obtained from the reaction of I and THQ with **1** at 50 °C. The structure of **6** consists of an isosceles triangle of osmium atoms with one elongated metal bond (Os(2)−Os(3) = 2.973(1) Å). The hydrides were located using the program HYDEX,[14] and as expected, the longer Os(2)−Os(3) bond

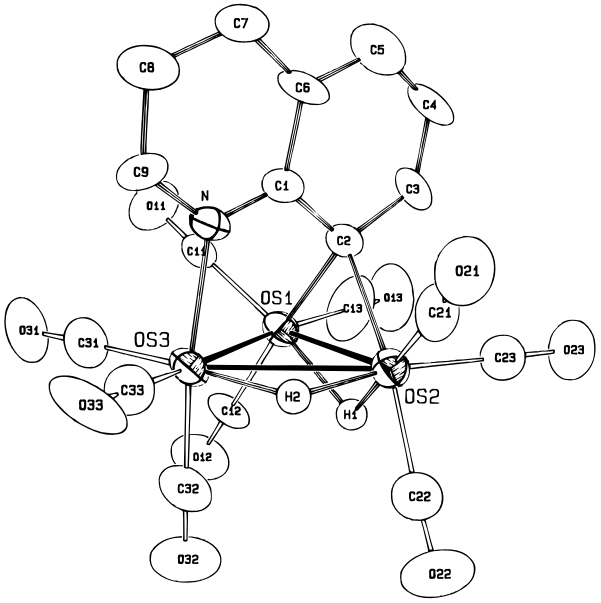

Figure 2. Solid-state structure of **6** showing the calculated positions of the hydrides.

has the more in plane hydride while the shorter doubly bridged Os(1)−Os(2) edge has the hydride tucked well below the plane of the metal triangle. These calculated positions for the hydrides are confirmed by the orientation of the carbonyl groups CO(11), CO(21), CO(31), and CO(23), essentially *trans* to the metal hydrogen bond vectors. The most interesting aspects of the structure of **6** are the carbon-nitrogen and carbon−carbon bond lengths. Thus, the N−C(1) bond length (1.30(2) Å) is clearly a carbon-nitrogen double bond and the C(1)−C(2) bond length (1.51(2) Å) is a carbon−carbon single bond. The somewhat shortened C(5)−C(6) and C(3)−C(4) bonds (1.38(3) and 1.32(2) Å) suggest more localized carbon−carbon double bonds, but the relatively large thermal ellipsoids for C(4) and C(6) and the intermediate bond lengths observed for C(4)−C(5) and C(2)−C(3) (1.43(3) and 1.47(2) Å) qualify this conclusion. It does seem clear, however, that aromaticity in the carbocyclic ring has been significantly disrupted and that the bonding of C(2) to the cluster is best viewed as an electron precise μ-alkylidene. This is further suggested by the symmetrical Os(1)−C(2) and Os(2)−C(2) interactions (both 2.18(2) Å).

The solid-state structure of **4** is shown in Figure 3, selected distances and bond angles are given in Table 4, atomic coordinates are in Table 5, and crystal data are in Table 1. The structure of **4** also consists of an isosceles triangle of osmium atoms with the elongated edge bridged by the more in plane hydride ligand and the shortest edge having the single atom amido bridge and a highly tucked hydrogen ligand. It is clear from the N−C(1) and C(1)−C(2) bond lengths (1.46(2) and 1.42(2) Å, respectively) that aromaticity has been restored to the carbocyclic ring. The C(1)−C(6) bond lengths fall into a much narrower range for **4** than for **6** overall (1.38(3)−1.42(3) Å *versus* 1.32(2)−1.51(2) Å) suggesting significant benzenoid character in the ring. As might be expected, the C(2)−Os(3) bond has shortened somewhat on becoming terminal (2.15(2) Å) while the N−Os(3) bond has become slightly elongated on becoming a bridging amido and exhibits a very slight

(14) Orpen, A. G. *J. Chem. Soc., Dalton Trans.* **1980**, 2509.

Table 1. Crystal Data for 6, 4, and 11

	compound		
	6	4	11
formula	$C_{18}H_{11}NO_9Os_3$	$C_{11}H_9NO_9Os_3$	$C_{19}H_9NO_9Os_3$
fw	955.89	941.86	968.92
crys dimens, mm^3	0.50 × 0.30 × 0.10	0.04 × 0.04 × 0.04	0.38 × 0.15 × 0.05
radiation, wavelength, Å	Mo, 0.710 73	Mo, 0.710 73	Mo, 0.710 73
temp, °C	25 ± 1	25 ± 1	20 ± 1
cryst system	monoclinic	orthorhombic	triclinic
space group	$P2_1/c$	$Pbca$	$P1$
a, Å	16.027(4)	15.082(5)	8.508(2)
b, Å	9.549(2)	16.391(5)	9.828(2)
c, Å	14.863(3)	16.777(3)	14.449(3)
α, deg			91.09(3)
β, deg	105.37(2)		106.88(3)
γ, deg			103.49(3)
V, $Å^3$	2193(2)	4147(3)	119.3(4)
Z	4	8	2
density, g/cm^3	2.89	3.02	2.88
abs coeff μ, cm^{-1}	174.1	184.2	170.33
rel transm coeff	0.210−0.999	0.751−0.949	0.520−0.999
scan type	$\omega-2\theta$	$\omega-2\theta$	$\omega-2\theta$
scan rate, deg/min	8.23	8.23	8.23
scan width, deg	0.8 + 0.350 tan(θ)	0.8 + 0.350 tan(θ)	0.8 + 0.350 tan(θ)
hkl ranges	h: −18 to 18	h: 0 to 19	h: −11 to 11
	k: 0 to 12	k: 0 to 20	k: −12 to 12
	l: 0 to 20	l: 0 to 21	l: −18 to 19
2θ range, deg	4.0−54.0	4.0−54.0	3.0−56.0
struct solution	Patterson method	Patterson method	Patterson method
no. of unique data	5063	5015	5391
no. of data used in LS refinement with $F_o > 4.0\sigma(F_o)$	2946	1998	4185
weighting scheme, w	$4F_o^2/[\sigma(F_o)^2]^2$	$4F_o^2/[\sigma(F_o)^2]^2$	$4F_o^2/[\sigma(F_o)^2]^2$
no. of params refined	280	271	248
R[a]	0.0499	0.0335	0.0696
R_w[b]	0.0630	0.0391	0.138
esd of obs of unit weight (GOF)	1.21	0.91	2.053
Largest shift/esd	0.05	0.01	−0.02
high peak in final diff map, e/A^3	0.92(45)	1.00(27)	5.54(45)

[a] $R = \Sigma\,||F_o| - |F_c||/\Sigma|F_o|$. [b] $R_w = [\Sigma w(F_o^2 - F_c^2)^2/\Sigma wF_o^4]^{1/2}$.

Table 2. Selected Bond Distances (Å) and Angles (deg) for 6[a]

Distances			
Os(1)−Os(2)	2.806(1)	C(1)−C(6)	1.46(2)
Os(1)−Os(3)	2.801(1)	C(2)−C(3)	1.47(2)
Os(2)−Os(3)	2.973(1)	C(3)−C(4)	1.32(2)
Os(1)−C(2)	2.18(2)	C(4)−C(5)	1.43(3)
Os(2)−C(2)	2.18(1)	C(6)−C(7)	1.51(3)
Os(3)−N	2.15(1)	C(7)−C(8)	1.45(3)
N−C(1)	1.30(2)	C(8)−C(9)	1.44(3)
N−C(9)	1.44(2)	Os−CO	1.91(2)[b]
C(1)−C(2)	1.51(2)	C−O	1.13(3)[b]
Angles			
Os(2)−Os(1)−Os(3)	64.04(2)	N−C(1)−C(2)	120.0(1)
Os(1)−Os(2)−Os(3)	57.89(2)	N−C(1)−C(6)	120.0(1)
Os(1)−Os(3)−Os(2)	58.07(2)	Os−C−O	177.0(2)[b]
Os(1)−C(2)−Os(2)	80.0(5)		

[a] Numbers in parentheses are estimated standard deviations. [b] Average values.

asymmetry. Since the colors, thermal behavior, and spectroscopic properties of **7** and **4** as well as **3** and **6** are so similar, we are certain that **3** and **4** are related to each other in the same way as **6** and **7**, as put forth above.

The solid-state structure of **11** is shown in Figure 4, selected distances and bond angles are given in Table 6, atomic coordinates are in Table 7, and crystal data are in Table 1. The structure of **11** consists of an isosceles triangle of Os atoms with the two hydride ligands located along the two longer Os−Os edges. The nitrogen atom derived from the μ-imino nitrogen of **8** (which in turn was derived from an acetonitrile ligand in **1**) now symmetrically caps the Os_3 triangle. Additionally, the THQ coordinated to the carbon atom of the former acetonitrile ligand has oxidatively added a C−H bond at the C(8) position. This results in the formation of a 2,4-diaza-1-metallacyclohexa-3-ene ring. Considering the C(1)−N(1) and C(1)−N(2) bond lengths of 1.39(2) and 1.34(2) Å, it is tempting to propose considerable delocalization over this three atom system. However, in order for **11** to be an electron precise $48e^-$

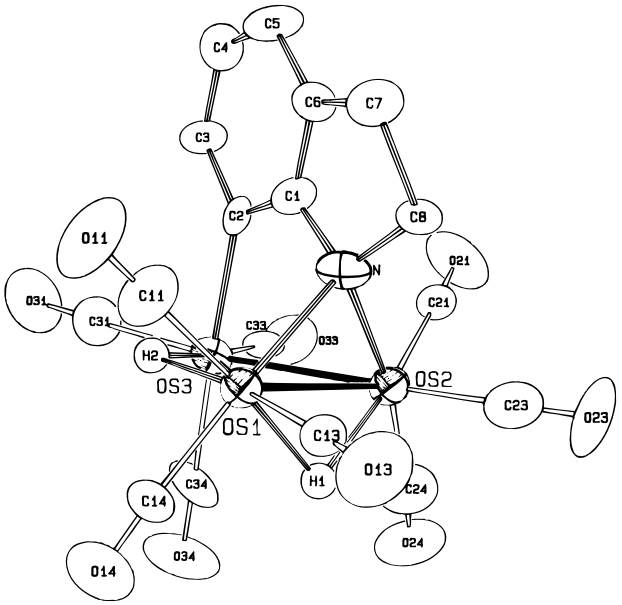

Figure 3. Solid-state structure of **4** showing the calculated positions of the hydrides.

Table 3. Positional Parameters and Their Estimated Standard Deviations for 6

atom	x	y	z
Os(1)	0.21542(4)	0.04448(7)	0.38285(4)
Os(2)	0.23167(5)	0.04649(6)	0.199943(4)
Os(3)	0.17209(4)	−0.20525(7)	0.28249(5)
O(11)	0.290(1)	−0.123(1)	0.5591(8)
O(12)	0.041(1)	0.074(2)	0.024(1)
O(13)	0.271(1)	0.335(1)	0.462(1)
O(21)	0.351(1)	−0.079(1)	0.0936(9)
O(22)	0.074(1)	0.108(2)	0.035(1)
O(23)	0.298(1)	0.340(1)	0.178(1)
O(31)	0.139(1)	−0.340(2)	0.456(1)
O(32)	−0.014(1)	−0.111(2)	0.213(1)
O(33)	0.1438(9)	−0.468(2)	0.162(1)
N	0.3090(9)	−0.246(1)	0.329(1)
C(1)	0.363(1)	−0.141(2)	0.342(1)
C(2)	0.329(1)	0.007(2)	0.331(1)
C(3)	0.397(1)	0.113(2)	0.355(1)
C(4)	0.481(1)	0.087(2)	0.378(1)
C(5)	0.512(1)	−0.054(2)	0.383(1)
C(6)	0.456(1)	−0.166(2)	0.366(1)
C(7)	0.491(1)	−0.313(2)	0.371(2)
C(8)	0.427(2)	−0.414(2)	0.382(2)
C(9)	0.337(1)	−0.390(2)	0.335(1)
C(11)	0.261(1)	−0.060(2)	0.496(1)
C(12)	0.106(1)	0.063(2)	0.409(1)
C(13)	0.250(2)	0.225(2)	0.433(1)
C(21)	0.305(1)	−0.030(2)	0.330(1)
C(22)	0.132(1)	0.079(2)	0.095(1)
C(23)	0.271(1)	0.231(2)	0.188(1)
C(31)	0.152(1)	−0.287(2)	0.392(1)
C(32)	0.056(1)	−0.149(2)	0.239(1)
C(33)	0.154(1)	−0.369(2)	0.206(1)
H(1)	0.162	0.123	0.268
H(2)	0.188	−0.133	0.173

Table 4. Selected Bond Distances (Å) and Angles (deg) for 4[a]

Distances			
Os(1)−Os(2)	2.795(1)	C(1)−C(6)	1.38(3)
Os(1)−Os(3)	3.019(1)	C(2)−C(3)	1.43(3)
Os(2)−Os(3)	2.818(1)	C(3)−C(4)	1.40(3)
Os(1)−N	2.15(1)	C(4)−C(5)	1.39(3)
Os(2)−N	2.18(2)	C(5)−C(6)	1.41(3)
Os(3)−C(2)	2.14(2)	C(6)−C(7)	1.52(3)
N−C(1)	1.46(2)	C(7)−C(8)	1.56(3)
N−C(8)	1.48(2)	Os−CO	1.94(2)[b]
C(1)−C(2)	1.42(3)	C−O	1.13(2)[b]

Angles			
Os(2)−Os(1)−Os(3)	57.85(3)	N−C(1)−C(2)	125.0(2)
Os(1)−Os(2)−Os(3)	65.07(3)	N−C(1)−C(6)	109.0(2)
Os(1)−Os(3)−Os(2)	57.08(3)	Os−CO	178.0(2)
Os(1)−N−Os(2)	80.0(2)		

[a] Numbers in parentheses are estimated standard deviations. [b] Average values.

cluster, a C(1)−N(1) single bond, a C(1)−N(2) double bond with a formal positive charge on N(2), and a formal negative charge on the metal triangle are required. This makes the capping nitrogen atom a formal five electron donor. This picture of the bonding mode is consistent with the lower range of infrared carbonyl stretching frequencies observed for **11** (2083−1944 cm^{-1}) compared with the other compounds reported here (2111−1970 cm^{-1}), as has been observed for other triosmium clusters bearing a formal negative charge.[15] The bond angles around C(1) and the coplanarity of the atoms around the C(1)−H(1) bond also support a formal C(1)−N(2) double bond.

D. Protonation of 3, 4, 6, and 7. In order to probe the electron distribution in the tautomeric pairs **3** and

(15) Kabir, S. E.; Day, M.; Irving, M.; McPhillips, T.; Minassian, H.; Rosenberg, E.; Hardcastle, K. I. *Organometallics* **1991**, *10*, 3997.

Table 5. Positional Parameters and Their Estimated Standard Deviations for 4

atom	x	y	z
Os(1)	0.11537(5)	0.12635(5)	0.08134(5)
Os(2)	0.20116(5)	−0.01421(5)	0.13556(5)
Os(3)	0.31358(5)	0.10459(5)	0.06819(5)
O(11)	0.073(1)	0.3022(9)	0.126(1)
O(13)	−0.076(1)	0.070(1)	0.103(1)
O(14)	0.087(1)	0.152(1)	−0.0950(9)
O(21)	0.346(1)	−0.059(1)	0.2557(9)
O(23)	0.0476(9)	−0.1160(9)	0.209(1)
O(24)	0.267(1)	−0.144(1)	0.017(1)
O(31)	0.423(1)	0.251(1)	0.016(1)
O(33)	0.4751(9)	−0.002(1)	0.102(1)
O(34)	0.288(1)	0.033(1)	−0.1000(9)
N	0.1564(9)	0.094(1)	0.2000(9)
C(1)	0.231(1)	0.143(1)	0.228(1)
C(2)	0.312(1)	0.155(1)	0.186(1)
C(3)	0.374(1)	0.206(1)	0.227(1)
C(4)	0.354(1)	0.24091)	0.301(1)
C(5)	0.272(1)	0.229(1)	0.338(1)
C(6)	0.209(1)	0.178(1)	0.300(1)
C(7)	0.113(1)	0.161(1)	0.321(1)
C(8)	0.093(1)	0.086(1)	0.267(1)
C(11)	0.091(1)	0.238(1)	0.109(1)
C(13)	−0.005(1)	0.090(1)	0.096(1)
C(14)	0.095(1)	0.145(1)	−0.029(1)
C(21)	0.291(1)	−0.043(1)	0.214(1)
C(23)	0.103(1)	−0.077(1)	0.181(1)
C(24)	0.240(2)	−0.099(1)	0.062(1)
C(31)	0.380(1)	0.198(1)	0.034(1)
C(33)	0.415(1)	0.037(1)	0.091(1)
C(34)	0.299(1)	0.057(1)	−0.039(1)
H(1)	0.133	0.019	0.045
H(2)	0.221	0.177	0.054

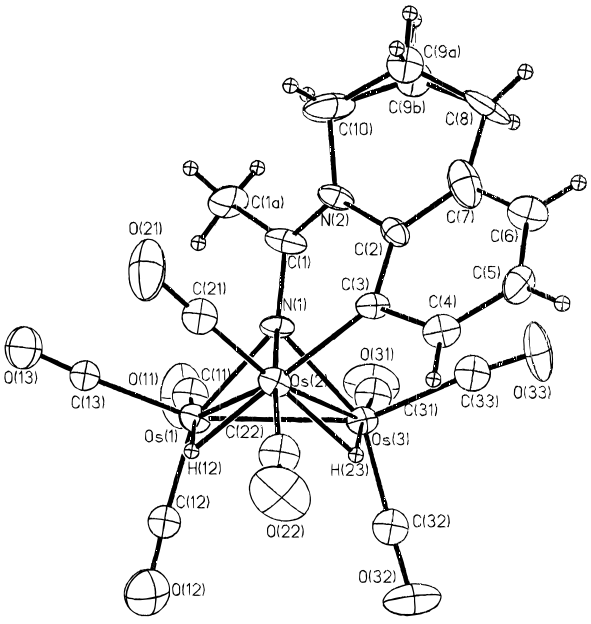

Figure 4. Solid-state structure of **11** showing the calculated position of the hydrides.

4 and **6** and **7**, we examined their protonation. The red tautomers **3** and **6** both protonate quantitatively with CF_3SO_3H in CD_2Cl_2. Protonation occurs at nitrogen as evidenced by the appearance of new broad resonances at 7.90 and 7.05 ppm, for **3** and **6**, respectively, which show COSY correlations with the aliphatic resonances of the nitrogen containing rings in **3** and **6**. These yellow solutions of $\mathbf{3}H^+$ and $\mathbf{6}H^+$ are stable indefinitely and, on reaction with base, deprotonate to regenerate the red complexes **3** and **6**. In sharp contrast, compound **7** protonates quantitatively at the metal core with CF_3SO_3H in CD_2Cl_2 as evidenced by the appearance of two

Table 6. Selected Bond Distances (Å) and Angles (deg) for 11[a]

Distances

Os(1)−Os(2)	2.842(1)	C(2)−C(3)	1.43(2)
Os(1)−Os(3)	2.721(1)	C(2)−C(7)	1.34(3)
Os(2)−Os(3)	2.864(1)	C(3)−C(4)	1.49(3)
Os(1)−N(1)	2.07(1)	C(4)−C(5)	1.40(3)
Os(2)−N(1)	2.09(1)	C(5)−C(6)	1.37(3)
Os(3)−N(1)	2.12(1)	C(6)−C(7)	1.44(3)
Os(1)−C(3)	2.01(2)	C(7)−C(8)	1.48(3)
C(1)−N(1)	1.39(2)	C(8)−C(9)	1.48(1)[b]
C(1)−N(2)	1.34(2)	C(9)−C(10)	1.48(1)[b]
C(2)−N(2)	1.41(2)	Os−CO	1.75(2)[c]
C(10)−N(2)	1.45(2)	C−O	1.14(2)[d]
C(1)−C(1A)	1.45(3)		

Angles

Os(1)−Os(2)−Os(3)	59.96(3)	N(1)−C(1)−C(1A)	116.0(2)
Os(1)−Os(3)−Os(2)	61.12(4)	N(1)−C(1)−N(2)	121.0(2)
Os(3)−Os(1)−Os(2)	61.92(4)	C(1)−N(2)−C(2)	125.0(1)
Os(1)−N(1)−Os(2)	86.2(5)	C(1)−N(2)−C(10)	115(2)
Os(1)−N(1)−Os(3)	81.1(4)	N(2)−C(2)−C(3)	119(2)
Os(2)−N(1)−Os(3)	85.9(5)	Os−C−O[c]	174.0(2)
C(2)−C(3)−Os(2)	124(5)		

[a] Numbers in parentheses are estimated standard deviations. [b] Average of C(8)−C(9A) and C(8)−C(9B), C(9A)−C(10) and C(9B)−C(10). [c] Average values.

Table 7. Atomic Coordinates and Their Standard Deviations for 11

	x	y	z
Os(1)	3718(1)	3655(1)	1975(1)
Os(2)	2256(1)	2934(1)	3492(1)
Os(3)	303(1)	2574(1)	1482(1)
O(11)	4044(25)	2961(23)	−6(11)
O(12)	4124(24)	6621(21)	1540(12)
O(13)	7403(20)	3783(17)	2976(10)
O(21)	5141(21)	2295(22)	4994(12)
O(22)	1865(29)	4921(20)	4984(13)
O(31)	113(26)	1476(17)	−550(10)
O(32)	−1305(28)	4947(18)	703(12)
O(33)	−3022(21)	399(21)	1338(14)
N(1)	2346(18)	1781(13)	2288(9)
N(2)	1595(20)	−463(14)	2865(9)
C(1)	2443(29)	392(18)	2360(12)
C(2)	330(22)	−164(17)	3231(11)
C(3)	567(23)	1222(17)	3664(11)
C(4)	−821(25)	1316(20)	4076(11)
C(5)	−2172(25)	161(33)	4038(14)
C(6)	−2182(29)	−1104(22)	3624(12)
C(7)	−898(29)	−1317(27)	3211(14)
C(8)	−1131(28)	−2764(19)	2803(17)
C(9A)	643(28)	−2856(34)	3201(27)
C(9B)	405(33)	−2875(45)	2562(35)
C(10)	2021(31)	−1802(22)	2992(18)
C(1A)	3734(27)	16(21)	2015(13)
C(11)	3868(30)	3052(24)	674(16)
C(12)	3999(26)	5428(22)	1717(13)
C(13)	6078(25)	3783(19)	2650(120
C(21)	3956(28)	2564(22)	4405(15)
C(22)	1976(32)	4214(27)	4419(17)
C(31)	88(29)	1826(24)	189(16)
C(32)	−632(28)	3977(23)	950(15)
C(33)	−1765(29)	1151(24)	1425(15)

new sharp hydride resonances at −16.00 and −13.83 ppm in a relative intensity of 2:1. On standing under N_2, this yellow solution of **7**H$^+$ gradually transforms to **6**H$^+$ as monitored by ^{1}H-NMR. Deprotonation of this solution with base yields a red solution which proved to contain **6** after chromatographic purification (Scheme 3). The same transformation occurs using a 4-fold excess of CF_3COOH, but the conversion is complete within 6 h.

E. Reaction of Tetrahydroisoquinoline with 1. The reaction of ITHQ with **1** in benzene at 50 °C yields a single product, $Os_3(CO)_{10}(\mu\text{-H})(\mu\text{-}\eta^2\text{-}C_9H_8N)$ (**13**), in

Scheme 3. Protonation and Interconversion of 6 and 7

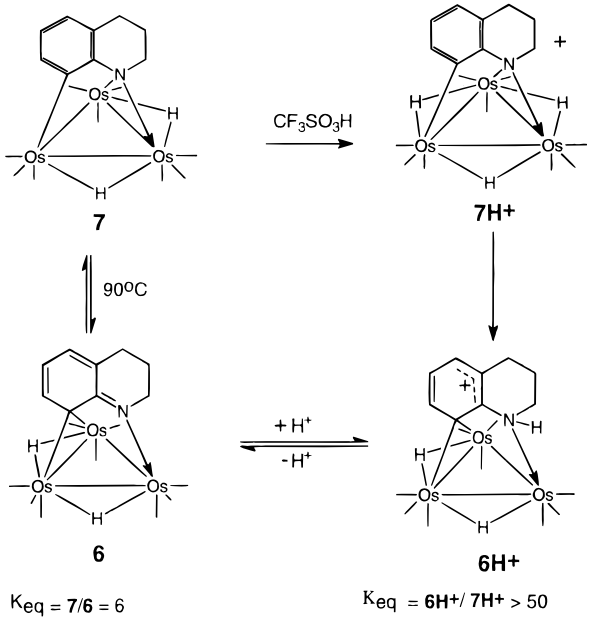

69% yield (eq 8). The structure is based on infrared,

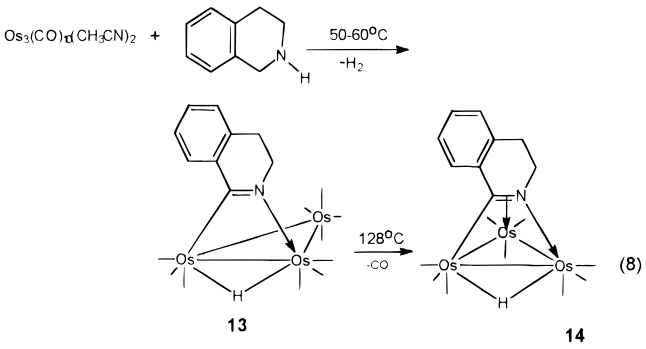

^{1}H-NMR, and elemental analysis and the similarity of its spectroscopic properties to related (μ-imidoyl)triosmium clusters.[10] Decarbonylation of **13** is readily accomplished either thermally or photochemically to yield $Os_3(CO)_9(\mu\text{-H})(\mu_3\text{-}\eta^2\text{-}C_9H_8N)$ (**14**; eq 8). As for **12**, a windshield wiper motion, typical of μ_3-imidoyl clusters, is observed. The low-temperature-limiting spectrum is obtained at −50 °C as for **12**.[10]

Discussion

The formation of compounds **2**−**7** where C−H activation is at the 7- and 8- positions of the indoline and tetrahydroquinoline ring, respectively, contrasts sharply with the results obtained by high-temperature reactions of these ligands with $Os_3(CO)_{12}$, where C−H activation at the 2-position is observed.[7] This is probably due to the availability of the binuclear reaction site potentiated by the presence of two relatively labile acetonitrile ligands combined with the higher reactivity of aromatic C−H bonds relative to aliphatic C−H bonds toward oxidative addition.[16] We have also observed C−H activation at the 8-position in the reaction of quinolines with **1**.[17] This essentially bimetallic reaction chemistry

(16) Jones, W. D.; Feher, F. J. *J. Am. Chem. Soc.* **1984**, *106*, 1650.
(17) Kabir, S. E.; Kolwaite, D. S.; Rosenberg, E.; Hardcastle, K. I.; Cresswell, W.; Grindstaff, J. *Organometallics* **1995**, *14*, 3611.

is apparently governed by electronic as well as geometric factors since ITHQ, where the aromatic C−H bonds are inaccessible to the cluster after initial nitrogen coordination, gives only **13** on reaction with **1** in which benzylic C−H bonds have been activated. Preferential activation of the aromatic and benzylic C−H bonds is most consistent with formation of a polarized (C^--H^+) interaction after dissociation of the second acetonitrile ligand has occurred. At higher temperatures and from a different intermediate (**8**), activation of sp^3 C−H bonds is also possible (**12**). On the other hand, the formation of **8** by an apparent direct nucleophilic attack by THQ on a coordinated acetonitrile suggests a tightly bound and polarized (C^+-N^-) nitrile ligand. We have also observed the formation of products analogous to **8** in the reactions of pyrrolidine with **1**.[18]

The conversion of **2** to **3** and **4** at 60 °C represents an unusually facile conversion of a decacarbonyl triosmium cluster containing a μ-coordinated ligand to the corresponding nonacarbonyl triosmium cluster containing a μ_3-coordinated ligand. For example, the related μ-imidoyl cluster **13** and related species undergo decarbonylation slowly at 128 °C.[19] Carbon−hydrogen activation with concomitant loss of a carbonyl group in μ-alkyne decarbonyl triosmium clusters takes place approximately 10 times slower than the conversion of **2** to **3** and **4**.[20] It is the back-reaction (carbonyl recapture) which adds to the sluggishness of these reactions and leads to significant deviations from first-order kinetics after about 1 half-life.[20] In the case of **2** converting to **3** and **4**, it seems reasonable to propose a proton transfer to the metal core from the amino N−H followed by amido-induced carbonyl dissociation. A related pyridine nitrogen induced carbonyl migration has recently been reported.[21] We did not observe the THQ analog of **2** even in the room-temperature reactions. Attempts to observe this intermediate by ^{1}H-NMR with CD_3CN solutions of **1** and THQ failed. The formation of **9** under such mild conditions indicates that dehydrogenation is a very facile process from the presumed intermediate analogous to **2** in the case of THQ. The thermolysis of **8** clearly shows that this complex is on a reaction pathway completely different from that of the major product **6**.

The tautomeric pairs **3** and **4** and **6** and **7** represent unusual examples of structures which differ very little in energy ($K_{eq} \sim 6$) but have a high kinetic barrier for interconversion. Clusters **3** and **6** both exhibit a much higher barrier for hydride migration than do **4** and **7**. Although we cannot point to a particular geometrical feature of the hydride geometries which accounts for this large difference in hydride mobility, we suggest here that it is the resulting overall cluster rigidity which accounts for the slow rates of tautomerization of **3** and **6** to **4** and **7**, respectively. We have previously noted that the rate of hydride exchange can have a significant influence on the course of organic ligand rearrangements and that relatively subtle changes in hydride geometry can have a dramatic influence on the rate of this exchange.[22]

The thermal behavior of **4** and **7** exhibits an interesting parallel with catalytic HDN. Whereas both **4** and **7** lose 1 mol of H_2 very slowly at 128 °C, bonding of the nitrogen to the metal is maintained in **7** while incorporation of the nitrogen lone pair into the indole π-system in **5** results in dissociation of the nitrogen from the metal. In catalytic HDN, indoles undergo much slower denitrification but more rapid hydrogenation than quinolines, and this has been attributed to weaker nitrogen metal binding and stronger π-aromatic binding of the indole ring to the catalytic surface.[23]

A second interesting feature, which bears strong resemblance to catalytic HDN, is the impact of protonation on the preferred bonding mode of the THQ moiety to the cluster. It has been known for some time that addition of protic acids to HDN catalyst systems enhances C−N bond cleavage.[4] This is thought to be the result of protonation at nitrogen which reduces C−N bond order making nucleophilic displacement by surface bound bases more favorable. The structures of **6** and **7** are very close in energy ($\Delta G° = 5$ kJ/mol) with **7** being the more stable form. Protonation effectively reverses this stability. The signal to noise on the ^{1}H-NMR spectrum of **7**H$^+$ after complete conversion to **6**H$^+$ was ~50:1, which means the equilibrium constant **6**H$^+$/**7**H$^+$ is at least 50 ($\Delta G° \geq 10$ kJ/mol). The proposed structure of **6**H$^+$ has reduced C−N bond order and disrupted aromaticity in the carbocyclic ring which may ultimately lead to cleavage of the C(10)−N bond by nucleophiles.

A systematic study of the hydrogenation of compounds **6, 7**, and **6**H$^+$ over a range of temperatures and hydrogen pressures, acidities, and solvents is currently underway in our laboratories. Initial results indicate that C−N bond cleavage to give 2-propylaniline results from hydrogenation of **7** but not for **6** and that **6**H$^+$ undergoes further reduction of the carbocyclic ring. The details of these studies will be reported separately.

Experimental Section

Materials. Compound **1** was synthesized by known literature procedures.[24] Indoline, tetrahydroquinoline, and tetrahydroisoquinoline were purchased from Aldrich and were vacuum distilled from CaH_2 directly before use. Benzene was distilled from sodium benzophenone ketyl, and methylene chloride and acetonitrile were distilled from CaH_2 directly before use. Trifluoromethanesulfonic acid and trifluoroacetic acid were purchased from Aldrich and used as received in a Braun drybox. NMR solvents were stored over molecular sieves (Mallincrodt 4A). Thin-layer chromatography was performed on 20 × 40 cm glass plates using a 2 mm layer of silica gel PF-254 (E&M Science). Two or three elutions were necessary to obtain adequate resolution of the bands. All reactions were performed under an atmosphere of prepurified nitrogen, but reactions were worked up in air. Elemental analyses were performed by Schwarzkopf Microanalytical.

Spectra. NMR spectra were obtained on a Unity Plus 400 NMR spectrometer, and infrared spectra were obtained on a Perkin-Elmer 1600 FT-IR.

Reaction of $Os_3(CO)_{10}(MeCN)_2$ with Indoline. (a) At Room Temperature. To a freshly distilled benzene solution (50 mL) of $Os_3(CO)_{10}(MeCN)_2$ (0.225 g, 0.241 mmol) was added indoline (203 μL, 1.81 mmol). The resulting mixture was

(18) Rosenberg, E.; Hardcastle, K. I. Unpublished results.
(19) Day, M.; Espitia, D.; Hardcastle, K. I.; Kabir, S. E.; Rosenberg, E.; Gobetto, R.; Milone, L.; Osella, D. *Organometallics* **1991**, *10*, 3550.
(20) Rosenberg, E.; Freeman, W.; Carlos, Z.; Yoo, Y.; Milone, L.; Gobetto, R. *J. Cluster Sci.* **1992**, *3*, 439.
(21) Deeming, A. J.; Smith, M. B. *J. Chem. Soc., Chem. Commun.* **1993**, 844.
(22) Rosenberg, E. In *The Synergy Between Dynamics and Reactivity of Clusters and Surfaces*; Farrugia, L. J., Ed.; Kluwer Academics: Dordrecht, The Netherlands, 1995; p 125.
(23) Ramirez de Agidelo, M. M.; Gallarraga, C.; Pimental, M. *Prepr., ACS Div. Pet. Chem.* **1993**, *38*, 700.
(24) Nicholls, J. N.; Vargas, M. D. *Inorganic Syntheses*; Kaesz, H. D., Ed.; Wiley Interscience: New York, 1989; p 292.

stirred at room temperature for 20 h. The solvent was removed under reduced pressure, and the residue was chromatographed by TLC on silica gel. Elution with hexane/CH_2Cl_2(10:3, v/v) gave one major and three very minor bands. The major band yielded $Os_3(CO)_{10}(\mu\text{-H})(\mu\text{-}\eta^2\text{-}C_8H_7NH)$ (**2**) as yellow crystals (0.156 g, 67%) from hexane/CH_2Cl_2 at −20 °C. The minor bands were too small for complete characterization.

Analytical and Spectroscopic Data for 2. Anal. Calcd for $C_{18}H_9NO_{10}Os_3$: C, 22.29; H, 0.94; N, 1.44. Found: C, 22.33; H, 0.71; N, 1.50. IR (ν(CO) in hexane): 2100 m, 2061 s, 2049 vs, 2020 s, 1998 s, 1992 sh, 1983 sh, 1973 w cm^{-1}. ^{1}H-NMR (C_6D_6): Major isomer (72%), 7.71 (d, 1H), 6.75 (dd, 1H), 6.47 (d, 1H), 4.15 (dd, br, 1H), 2.35 (m, 2H), 1.85 (m, 2H), −13.59 (s, 1H) ppm; minor isomer (28%), 7.61 (d, 1H), 6.66 (dd, 1H), 6.29 (d, 1H), 4.05 (br, 1H), 2.35 (m, 2H), 1.85 (m, 2H), −13.80 (s, 1H) ppm.

At 50−60 °C. To a freshly distilled benzene solution (200 mL) of $Os_3(CO)_{10}(MeCN)_2$ (0.400 g, 0.429 mmol) was added indoline (213 μL, 1.90 mmol). The reaction mixture was heated at 50−60 °C for 8 h. The solvent was rotary evaporated, and the residue was chromatographed by TLC on silica gel. Elution with hexane/CH_2Cl_2 (10:3, v/v) gave two major bands and two very minor bands. The faster moving red band yielded $Os_3(CO)_9(\mu\text{-H})_2(\mu_3\text{-}\eta^2\text{-}C_8H_7N)$ (**3**) as red crystals (0.121 g, 30%) from hexane/CH_2Cl_2 at −20 °C. The slower moving yellow band gave $Os_3(CO)_9$ $(\mu\text{-H})_2(C_8H_7N)$ (**4**) as yellow crystals (0.090 g, 22%) from hexane/CH_2Cl_2 at −20 °C. The minor bands were too small for complete characterization.

Analytical and Spectroscopic Data for 3 and 4. Data for **3** are as follows. Anal. Calcd for $C_{17}H_9NO_9Os_3$: C, 21.68; H, 0.97; N, 1.49. Found: C, 21.58; H, 0.88; N, 1.66. IR (ν(CO) in hexane): 2099 m, 2072 s, 2045 s, 2022 s, 2018 sh, 2000 m, 1991 m, 1973 m cm^{-1}. ^{1}H-NMR ($CDCl_3$): 6.79 (d, 1H), 6.45 (d, 1H), 3.65 (m, 1H), 3.46 (m, 1H), 2.84 (m, 2H), −13.21 (d, 1H), −13.32 (d, 1H) ppm. Data for **4** are as follows. Anal. Calcd for $C_{17}H_9NO_9Os_3$: C, 21.68; H, 0.97; N, 1.49. Found: C, 21.77; H, 0.92; N, 1.55 IR (ν(CO) in hexane): 2012 m, 2078 s, 2047 vs, 2037 s, 2027 m, 2008 m, 1991 m, 1974 m, cm^{-1}. ^{1}H-NMR (CD_2Cl_2, −50 °C): 7.21 (d, 1H), 6..61 (d, 1H), 6.51 (dd, 1H), 3.88 (m, 1H), 3.46 (m, 1H), 3.19 (m, 1H), 2.92 (m, 1H), −13.80 (s, 1H), −13.92 (s, 1H) ppm.

Thermolysis of $Os_3(CO)_9(\mu\text{-H})_2(\mu_3\text{-}\eta^2\text{-}C_8H_7N)$ (3 or 4). An octane solution of $Os_3(CO)_9(\mu\text{-H})_2(\mu_3\text{-}\eta^2\text{-}C_8H_7N)$ (0.100 g, 0.106 mmol) was heated to reflux for 7 h. The solvent was removed *in vacuo*, and the residue was chromatographed by TLC on silica gel. Elution with hexane/CH_2Cl_2 (10:3, V/V) gave three bands. The red band gave unconsumed **3** (0.038 g, 38%). The yellow band afforded **4** (0.042 g, 42%). The slower moving colorless band gave $Os_3(CO)_9(\mu\text{-H})_2(\mu_3\text{-}\eta^2\text{-}C_8H_4NH)$ (**5**) (0.015 g, 15%). Longer reflux times led to considerable nonspecific decomposition. The compound gave ^{1}H-NMR and IR spectra identical with those previously reported for **5**.[12]

Reaction of $Os_3(CO)_{10}(MeCN)_2$ with 1,2,3,4-Tetrahydroquinoline. 1,2,3,4-Tetrahydroquinoline (269 μL, 2.15 mmol) was added to freshly distilled benzene or CH_2Cl_2 solution (200 mL) of $Os_3(CO)_{10}(MeCN)_2$ (0.400 g, 0.429 mmol). The reaction mixture was heated at 50−60 °C for 8 h (for benzene) or refluxed overnight for CH_2Cl_2. Stirring benzene solutions of **1** with tetrahydroquinoline at room temperature gave approximately the same product distribution. Chromatographic separation as above gave four bands from which the following compounds were isolated (in order of elution): a yellow band of $Os_3(CO)_{10}(\mu\text{-H})(\mu\text{-}\eta^2\text{-}C_9H_6N)$ (**9**) (0.17 g, 7%);[17] a yellow band of $Os_3(CO)_{10}(\mu\text{-H})(\mu\text{-}\eta^1\text{-}C_9H_{10}N(CH_3)CN)$ (**8**) as yellow-orange crystals (0.031 g, 12%) from hexane/CH_2Cl_2 at −20 °C; a third red band of $Os_3(CO)_9(\mu\text{-H})_2(\mu_3\text{-}\eta^2\text{-}C_9H_9N)$ (**6**) as red crystals (0.126 g, 31%) from hexane/CH_2Cl_2 at −20 °C; a fourth yellow band of $Os_3(CO)_9$ $(\mu\text{-H})_2(\mu_3\text{-}\eta^2\text{-}C_9H_9N)$ (**7**) as yellow crystals (0.036 g, 9%) from hexane/CH_2Cl_2 at −20 °C. Several other bands were noted but were not isolated in sufficient yield to fully characterize.

Analytical and Spectroscopic Data for 6 and 7. Data for **6** are as follows. Anal. Calcd for $C_{18}H_{11}NO_9Os_3$: C, 22.62; H, 1.16; N, 1.47. Found: C, 22.60; H, 0.99; N, 1.19. IR (ν(CO) in hexane): 2099 m, 2072 s, 2044 s, 2022 s, 2018 m, 2000 m, 1989 w, 1972 w cm^{-1}. ^{1}H-NMR (400 MHz) (in $CDCl_3$): 6.80 (d, 1H), 6.63 (d, 1H), 5.42 (dd, 1H), 3.12 (dt, 1H), 3.35 (dd, 1H), 2.52 (t, 2H), 1.57 (m, 2H), −12.98 (d, 1H), −13.88 (d, 1H) ppm. ^{13}C-NMR ($CDCl_3$) hydrocarbon region (ppm): C(8), 195.72; CH-(7), 163.34; CH(6), 111.97; CH(5), 131.44; C(10), C(9), 129.45; C(10), 42.5; CH_2(2), 62.91; CH_2(3), 23.80; CH_2(4), 27.73. ^{13}C-NMR ($CDCl_3$) carbonyl region: 163.26 (1C), 165.68 (1C), 170.91 (1C), 172.95 (1C), 174.68 (1C), 176.07 (1C), 178.10 (1C), 180.65 (1C), 185.48 (1C) ppm. Data for **7** are as follows. Anal. Calcd for $C_{18}H_{11}NO_9Os_3$: C, 22.62; H, 1.16; N, 1.47. Found: C, 22.62; H, 1.08; N, 1.47. IR (ν(CO) in hexane): 2111 w, 2078 s, 2048 s, 2038 m, 2025 m, 2008 m, 1991 w, 1973 w cm^{-1}. ^{1}H-NMR (400 MHz) (in CD_2Cl_2 at −80 °C): 7.25 (d, 1H), 6.35 (dd, 1H), 6.38 (d, 1H), 3.92 (dd, 1H), 3.30 (dd, 1H), 2.91 (m, 1H), 2.47 (dd, 1H), 1.84 (m, 1H), 1.63 (m, 1H), −13.70 (s, 1H), −13.90 (s, 1H) ppm. ^{13}C-NMR (CD_2Cl_2): CH(7) 142.06, CH(6) 124.20, CH(5) 123.14, C(10) 126.57, C(9) 125.38, CH_2(2) 82.79, CH_2(3) 28.35, CH_2(4) 26.76 ppm. ^{13}C-NMR (CD_2Cl_2): carbonyl region, 161.58 (1C), 163.39 (1C), 168.17 (1C), 169.50 (1C), 173.67 (1C), 175.49 (1C), 177.55 (1C), 178.08 (1C), 184.19 (1C) ppm.

Analytical and Spectroscopic Data for 8. Anal. Calcd for $C_{21}H_{14}N_2O_{10}Os_3$: C, 24.61; H, 1.38; N, 2.73. Found: C, 24.79; H, 1.33; N, 2.66. IR (ν(CO) in hexane): 2100 m, 2063 vs, 2050 vs, 2034 m, 2018 vs, 2003 vs, 1991 s, 1977 w cm^{-1}. ^{1}H-NMR (400 MHz) (in $CDCl_3$): 7.10 (d, 1H), 7.00 (dd, 1H), 6.82 (dd, 1H), 5.95 (d, 1H), 3.65 (m, 2H), 2.87 (m, 2H), 2.58 (s, 3H), 2.05 (dm, 2H), −15.07 (s, 1H). ^{13}C-NMR ($CDCl_3$), hydrocarbon region (ppm): Acetonitrile C, 170.66; C(10), 141.26; CH, 130.01; CH, 126.79; C(9), 124.43; CH, 120.40; CH, 115.66; CH_2, 46.89; CH_3, 27.28; CH_2, 26.79; CH_2, 21.94. ^{13}C-NMR ($CDCl_3$), carbonyl region (ppm): 185.36 (1C), 180.38 (1C), 178.15 (1C), 178.12 (1C), 175.32 (1C), 175.27 (1C), 173.09 (1C), 173.05 (1C), 168.08 (2C) ppm.

Spectroscopic data for **9** were identical with that previously reported for the same compound synthesized from the reaction of **1** with Q.[17]

Thermolysis of $Os_3(CO)_9(\mu\text{-H})_2(\mu_3\text{-}\eta^2\text{-}C_9H_9N)$ (7). A 30.0 mg amount of compound **1** was dissolved in 25 mL of octane and refluxed overnight under an atmosphere of nitrogen. The reaction mixture was rotary evaporated and the residue purified by thin-layer chromatography to yield 11.0 mg (23%) of a single product in addition to nonspecific decomposition. The ^{1}H-NMR, 2D-^{1}H-COSY, and infrared are consistent with the formulation $(\mu\text{-H})Os_3(CO)_{10}(\mu\text{-}\eta^2\text{-}C_9H_9N)$ (**10**).

Analytical and Spectroscopic Data for 10. Anal. Calcd for $C_{19}H_9NO_{10}Os_3$: C, 23.67; H, 0.95; N, 1.47. Found: C, 22.93; H, 0.84; N, 1.06. IR (ν(CO) in hexane): 2077 m, 2061 m, 2047 vs, 2021 s, 1990 m, br. ^{1}H-NMR ($CDCl_3$): 8.85 (dd, 1H), 8.22 (d, 1H), 7.83 (d, H), 6.80 (dd, 1H), 3.10 (m, 2H), 2.85 (m, 2H), −13.01 (s, 1H) ppm.

Thermolysis of $Os_3(CO)_{10}(\mu\text{-H})(\mu\text{-}C_9H_{10}N(CH_3CN))$ (8). An octane (25 mL) solution of **8** (0.050 g, 0.049 mmol) was heated to reflux for 24 h. After cooling, the solvent was rotary evaporated and the residue was chromatographed by TLC on silica gel. Elution with hexane/CH_2Cl_2 (10:3, v/v) gave three bands from which the following compounds were isolated (in order of elution): $Os_3(\mu\text{-H})(CO)_9(\mu\text{-}\eta^2\text{-}C_9H_8N)$ (**12**, 0.012 g, 23%); unconsumed **8** (0.010 g); $Os_3(CO)_8(\mu\text{-H})_2(\mu\text{-}C_9H_9N(CH_3\text{-}CN))$ (**11**) as yellow crystals (0.022 g, 45%) from hexane/CH_2Cl_2 at −20 °C.

Spectroscopic and Analytical Data for 11. Anal. Calcd for $C_{19}H_{14}O_8N_2Os_3$: C, 23.55, H, 1.45, N, 2.89. Found: C, 22.98, H, 1.97, N, 3.12. IR (ν(CO) in hexane/CH_2Cl_2): 2083 s, 2049 vs, 2013 s, 1992 s, br, 1944 m, br cm^{-1}. ^{1}H-NMR (400 MHz) (in $CDCl_3$): 7.93 (d, 1H), 6.96 (dd, 1H), 6.83 (d, 1H), 4.29 (m, 1H), 3.57 (m, 1H), 2.94 (m, 1H), 2.88 (s, 3H), 2.78 (m, 1H), 2.08 (m, 2H), −16.95 (s, 1H), −17.67 (s, 1H) ppm.

Spectroscopic Data for 12. IR (ν(CO) in hexane): 2092 m, 2065 s, 2040 s, 2013 s, 2001 m, 1994 s, 1987 w, 1983 w, 1970 w cm^{-1}. ^{1}H-NMR (400 MHz) (in $CDCl_3$, −50 °C): 7.49

(d, 1H), 7.34 (dd, 1H), 7.28 (dd, 1H), 6.98 (d, 1H), 3.71 (dt, 1H), 3.35 (dd, 1H), 2.83 (dt, 1H), 2.69 (dd, 1H), −17.2 (s, 1H) ppm.

Kinetics of Conversion of 2 to 3 and 4, 3 to 4, and 6 to 7. Solutions of **2, 3**, or **6** (0.04 mmol) in 0.6 mL of C_6D_6 or $C_6D_5CD_3$ were inserted into a thermostated 5 mm NMR probe at 60, 90, and 100 °C respectively, and a ^{1}H-NMR spectrum was taken every 1 h for ∼15 h. Approximately 90 s elapsed between the sample insertion and the first accumulation. Each accumulation took 96 s (32 transients, acquisition time = 2 s, relaxation delay = 1 s). The rate constants for the conversions of **2** to **3** and **4**, **3** to **4**, and **6** to **7** were evaluated by measuring the relative intensities of each isomer. The k_{obs} for these conversions was calculated using the Varian analysis programs "kind" and "kini" which fits the measured intensities to the eq $I_o = Ie^{-t/\tau} + I_\infty$. The calculated value of τ is the inverse of the first-order rate constant in seconds. The errors reported are ±10% on the basis of the expected error in relative integrated intensities for the NMR technique (±5%).

Protonation of 3, 6, and 7. Solutions of **3**, **6**, or **7** (∼0.04 mmol) in 0.6 mL of CD_2Cl_2 in a 5 mm NMR tube were treated with 1 μL CF_3SO_3H or 5 μL of CF_3COOH. The deep red solutions of **3** and **6** turned lemon yellow, while the yellow-orange solution of **7** lightened slightly. The solutions were monitored for two days by ^{1}H-NMR during which time the solution of **7**H$^+$ converted completely to **6**H$^+$ while the solutions of **3**H$^+$ and **6**H$^+$ were stable indefinitely. Treatment of **3**H$^+$ and **6**H$^+$ with $Li^+Et_3BH^-$ regenerated **3** and **6** after chromatographic purification. ^{1}H-NMR for **3**H$^+$ (CD_2Cl_2): 8.06 (d, 1H), 7.98 (d, 1H), 7.91 (s, br, 1H), 6.92 (dd, 1H), 4.12 (m, 1H), 3.96 (m, 1H), 3.34 (m, 1H), 3.21 (m, 1H), −13.79 (s, 1H), −14.61 (s, 1H) ppm. ^{1}H-NMR for **6**H$^+$ (CD_2Cl_2): 7.95 (d, 1H), 7.85 (d, 1H), 7.00 (d, br, 1H), 6.81 (dd, 1H), 3.38 (dd, 1H), 3.22 (m, 1H), 3.15 (m, 2H), 1.98 (m, 1H), 1.80 (m, 1H), −12.95 (d, 1H), −14.92 (d, 1H) ppm. ^{1}H-NMR for **7**H$^+$(CD_2Cl_2): 7.21 (m, 1H), 6.63 (m, 2H), 4.00 (m, 2H), 2.95 (m, 2H), 1.95 (m, 2H) −13.83 (s, 1H), −16.00 (s, 2H) ppm.

Reaction of $Os_3(CO)_{10}(CH_3CN)_2$ (1) with Tetrahydroisoquinoline. To a solution of 0.350 mg (0.38 mmol) of **1** in 150 mL of benzene was added 142 μL (1.1 mmol) of tetrahydroisoquinoline. The reaction mixture was heated for 6h at 50 °C under nitrogen at which time analytical TLC indicated that all of **1** had been consumed. The reaction mixture was rotary evaporated to dryness, taken up in CH_2Cl_2, and purified by thin-layer chromatography to yield one major yellow band, 240 mg (69%) of $Os_3(CO)_{10}(\mu\text{-H})(\mu\text{-}\eta^2\text{-}C_9H_8N)$ (**13**).

Analytical and Spectroscopic Data for 13. Anal. Calcd for $C_{19}H_9NO_{10}Os_3$: C, 23.24; H, 0.92, N, 1.43. Found: C, 23.32; H, 0.85; N, 1.46. IR (ν(CO) hexane): 2100 m, 2058 s, 2048 s, 2021 s, 2006, 2000 sh, 1986 m, br, 1972 w. ^{1}H-NMR ($CDCl_3$): 7.57 (d, 1H), 7.39 (m, 2H), 7.07 (d, 1H), 3.61 (m, 2H), 2.69 (m, 2H), −15.02 (s, 1H) ppm.

Thermolysis of $Os_3(CO)_{10}(\mu\text{-H})(\mu\text{-}\eta^2\text{-}C_9H_8N)$ (13). A 138 mg (0.14 mmol) amount of **13** was combined with 30 mL of octane, and the reaction mixture was refluxed for 12 h under nitrogen. The solution was rotary evaporated, and purification by thin-layer chromatography gave two bands; one band proved to be recovered **13** and the second band proved to be $Os_3(CO)_9(\mu\text{-H})(\mu_3\text{-}\eta^2\text{-}C_9H_8N)$ (**14**), 65 mg (73%, based on consumed **13**).

Analytical and Spectroscopic Data for 14. Anal. Calcd for $C_{18}H_9O_9Os_3$: C, 22.67; H, 0.94; N, 1.47. Found: C, 22.69; H, 0.81; N, 1.58. IR (ν(CO), hexane): 2088 m, 2061 s, 2037 s, 2010 s, 1990 m, br, 1969 m. ^{1}H-NMR (CD_2Cl_2, −50 °C): 7.58 (d, 1H), 7.34 (m, 2H), 7.04 (d, 1H), 3.70 (m, 1H), 3.35 (m, 1H), 2.72 (m, 2H), −17.16 (s, 1H) ppm.

X-ray Structure Determination of 4, 6, and 10. Crystals of **4, 6**, and **11** for X-ray examination were obtained from saturated solutions of each in hexane/dichloromethane solvent systems at −20 °C. Suitable crystals of each were mounted on glass fibers, placed in a goniometer head on the Enraf-Nonius CAD4 diffractometer, and centered optically. Unit cell parameters and an orientation matrix for data collection were obtained by using the centering program in the CAD4 system. Details of the crystal data are given in Table 1. For each crystal, the actual scan range was calculated by scan width = scan range + 0.35 tan θ and backgrounds were measured by using the moving-crystal−moving-counter technique at the beginning and end of each scan. Two or three representative reflections were monitored every 2 h as a check on instrument and crystal stability, and an additional two reflections were monitored periodically for crystal orientation control. Lorentz, polarization, and decay corrections were applied, as was an empirical absorption correction based on a series of Ψ scans, for each crystal. The weighting scheme used during refinement was $1/\sigma^2$, based on counting statistics.

Each of the structures was solved by the Patterson method using SHELXS-86,[25] which revealed the positions of the metal atoms. All other non-hydrogen atoms were found by successive difference Fourier syntheses. The expected hydride positions were calculated by using the program HYDEX,[14] and hydrogen atoms were included in **11** and were placed in their expected chemical positions using the program HYDRO.[26] The hydrides were given fixed positions and U's in each structure while the hydrogens in **11** were included as riding atoms in the final least-squares refinements with U's which were related to the atoms ridden upon. All other non-hydrogen atoms were refined anisotropically in each of the structures.

The ADP's of carbons 8 and 9 of **10** indicated the presence of positional disorder in that part of the ligand, so we attempted to model that disorder. There is an approximately 60:40 mixture of conformational isomers occupying equivalent sites in the crystal lattice. Apparently, there are no strong intermolecular interactions to favor the specific crystallization of one conformer or the other, uniquely, in the crystal lattice.

Scattering factors were taken from Cromer and Waber.[27] Anomalous dispersion corrections were those of Cromer.[28] All data processing was carried out on a DEC MicroVAX II computer using the MOLEN system of programs. Structure solution, refinement, and preparation of figures and tables for publication were carried out on a DEC MicroVAX II using SHELXS-86[25] and MOLEN[26] for **4** and **6**, while, for **11**, the structure was completed using a PC and the SHELXL-93[29] and XP/PC[30] programs.

Acknowledgment. We gratefully acknowledge the National Science Foundation (E.R., Grant CHE9319062) for research support and for an instrument grant (CHE9302468) for purchase of a 400 MHz NMR.

Supporting Information Available: Tables 8−14, listing complete bond distances and angles, anistropic displacement parameters, and H parameters for **6**, **4**, and **11**, respectively (17 pages). Ordering information is given on any current masthead page.

OM9507235

(25) Sheldrick, G. M. *Acta Crystallogr.* Kynoch: Birmingham, U.K., **1990**, *A46*, 467.
(26) Fair, C. K. *MolEN Structure Determination System*; Enraf-Nonius: Delft, The Netherlands, 1990.
(27) Cromer, D. T.; Waber, J. T. *International Tables for X-ray Crysallography*; Kynoch: Birmingham, U.K., 1974; Vol. 4, Table 2.2B.
(28) Cromer, D. T. *International Tables for X-ray Crystallography*; Kynoch: Birmingham, U.K., 1990; Vol. 4, Table 2.3.1.
(29) Sheldrick, G. M. *Program for Structure Refinement*; University of Goettingen: Goettingen, Germany, 1993.
(30) *XP/PC, Molecular Graphics Software*; Siemans Analytical X-ray Instruments, Inc.: Madison, WI.